

Electronic supplementary information for

Oxygen-Doped Hollow Porous NiCoP Nanocages Derived from Ni-Co Prussian Blue Analog for Oxygen Evolution

Di Li^a, Changjian Zhou^a, Yingying Xing^a, Xiangli Shi^a, Wanxia Ma^b, Longhua Li^b, Deli Jiang^{b,}, and Weidong Shi^{b,*}*

^aInstitute for Energy Research, Jiangsu University, Zhenjiang 212013, China

^bSchool of Chemistry and Chemical Engineering, Jiangsu University, Zhenjiang 212013, China

Corresponding Author: dlj@ujs.edu.cn (D. J.), swd1978@ujs.edu.cn (W. S.)

Materials.....	3
Synthesis of Ni-Co PBA Nanocubes.....	3
Synthesis of Ni-Co PBA Nanocages.....	3
Synthesis of Ni-Co PBA Derived Phosphides	4
Synthesis of Oxygen Doped Ni-Co Metal Phosphides	4
Structural Characterization.....	4
Electrochemical Measurements	5
Density Functional Theory (DFT) Calculations	5
FIGURES	7
Fig. S1 SEM and TEM images of NiCoPBA Cubes.	7
Fig. S2 N ₂ adsorption-desorption isotherms and pore size distribution for NiCoP Cubes and O-NiCoP Cages	8
Fig. S3 (a) XRD patterns of NiCoPBA and other derivative catalysts. (b) FT-IR spectra of NiCoPBA Cages and O-NiCoP Cages.....	9
Fig. S4 XPS spectra of NiCoP Cages and O-NiCoP Cages.....	10
Fig. S5 The LSV curves of O-NiCoP Cages-1h and O-NiCoP Cages-3h samples.	11
Fig. S6 Polarization curves normalized by the ECSA.	12
Fig. S7 CVs of sample (a) NiCoPBA Cubes, (b) NiCoPBA Cages, (c) NiCoP Cubes, (d) NiCoP Cages, (e) O-NiCoP Cubes, and (f) O-NiCoP Cages.....	13
Fig. S8 A digital photograph showing the continuous generation of O ₂ bubbles on the O-NiCoP Cages catalyst.....	15
Fig. S9 SEM and TEM images of O-NiCoP Cages after OER test.	16
Fig. S10 XPS spectra of O-NiCoP Cages after OER test.	17
Fig. S11 Simulated OER steps proceeded	18
Table S1 Summary of electrochemical OER performance of previously reported metal phosphide.	19

EXPERIMENTAL SECTION

Materials

Nickel (II) chloride hexahydrate ($\text{NiCl}_2 \cdot 6\text{H}_2\text{O}$), sodium citrate ($\text{C}_6\text{H}_5\text{Na}_3\text{O}_7 \cdot 2\text{H}_2\text{O}$), potassium hydroxide (KOH), and absolute ethanol were purchased from Sinopharm Chemical Reagent Co., Ltd. (Shanghai, China). Potassium hexacyanocobaltate (III) ($\text{K}_3[\text{Co}(\text{CN})_6]_2$) was bought from Macklin Biochemical Co., Ltd. (Shanghai, China), ruthenium oxide (RuO_2 , 5 wt%) was commercial products obtained from Aladdin (Shanghai, China). Nafion perfluorinated resin solution (5 wt%) was bought from Sigma-aldrich Co. (USA). All chemical reagents can be used directly and deionized water was used throughout the experiment.

Synthesis of Ni-Co PBA Nanocubes

Ni-Co PBA nanocubes (NiCoPBA Cubes) were synthesized through a coprecipitation approach.¹ Typically, 0.1330 g of $\text{K}_3[\text{Co}(\text{CN})_6]_2$ was dissolved in 20 mL deionized water and stirred to form a solution (solution A). 0.1426 g of $\text{NiCl}_2 \cdot 6\text{H}_2\text{O}$ and 0.2353 g of $\text{C}_6\text{H}_5\text{Na}_3\text{O}_7 \cdot 2\text{H}_2\text{O}$ were added into 20 mL deionized water and generated a clear solution B. Then, solution A and solution B were mixed for 7 days under stirring. The as-prepared precipitate was alternatively washed with ethanol and deionized water three times, and dried in a vacuum at 60 °C, then the final gray blue sample can be obtained.

Synthesis of Ni-Co PBA Nanocages

5 mL ammonia was added into 20 mL deionized water and then dropwise added 10 mL absolute ethyl alcohol containing 20 mg of PBA precursor, and stirred for 90 min at room temperature. The precipitate was centrifuged, washed with water and alcohol and dried at 60 °C to obtain nanocage structure. To study the formation process of Ni-Co PBA nanocages (NiCoPBA Cages), the stirring time was changed from 30 to 60 min while other experimental

conditions unchanged.

Synthesis of Ni-Co PBA Derived Phosphides

NaH₂PO₂·H₂O was placed on the upstream side of the tube furnace and the obtained NiCoPBA Cages were placed in the middle of the tube furnace and the mass ratio of the NaH₂PO₂·H₂O and NiCoPBA Cages is 5:1. Subsequently, the product was heat to 300 °C at a heating rate of 2 °C min⁻¹ and hold for 2 h under a N₂ atmosphere and the obtained product named NiCoP Cages. For comparison, the as-prepared NiCoP Cubes were obtained under the same experimental conditions by changing the NiCoPBA Cages to NiCoPBA Cubes.

Synthesis of Oxygen Doped Ni-Co Metal Phosphides

The as-prepared NiCoP Cages were annealed at 350 °C for 2 h with a heating rate of 2 °C min⁻¹ in air and the product named O-NiCoP Cages. The NiCoP Cages annealed for 1 h and 3 h (the products were named as O-NiCoP Cages-1h and O-NiCoP Cages-3h) were used as the control experiments. In addition, for comparison, the as-prepared NiCoP Cubes were annealed to prepare O-NiCoP Cubes under the same experimental conditions.

Structural Characterization

The constituent of synthesized catalyst was tested by X-ray diffraction (Bruker D8 Advance Cu K α radiation; $\lambda = 1.5406 \text{ \AA}$) at a scan rate of 7° min⁻¹ between 10° and 80°. Scanning electron microscope (SEM, S-4800 II FESEM, 15 kV), transmission electron microscope (TEM, Tecnai 12, 120 kV) and high-resolution TEM (HRTEM, Tecnai G2 F30 S-Twin TEM, 300 kV) were used to characterize the morphology and structure. X-ray photoelectron spectroscopy (XPS, ESCA PHI500 spectrometer) was operated with an Al K α radiator to analyze the surface composition. TriStar II 3020-BET/BJH surface area (BET)

was used to characterize the specific surface area and porous structure of the catalyst.

Electrochemical Measurements

All electrochemical tests were performed using CHI-760E electrochemical workstation. The three-electrode device is composed of a reference electrode (Ag/AgCl electrode), a counter electrode (a platinum wire) and a working electrode (the prepared electrocatalyst). According to the equation of $E_{\text{RHE}} = E_{\text{Ag/AgCl}} + 0.197 \text{ V} + 0.059 \times \text{pH}$, all the measured potentials are calibrated to the reversible hydrogen electrode (RHE) scale. 4 mg catalyst was dissolved in a mixture contained 960 μL ethanol and 40 μL nafion. After 30 minutes of ultrasound, 5 μL catalyst mixture was dropped onto a 3 mm glassy carbon electrode followed by drying at room temperature naturally. In 1 M KOH alkaline solution, LSV test was performed at a scanning rate of 2 mV S^{-1} , electrochemical impedance spectroscopy (EIS) measurements were performed in the frequency range of 0.01 to 10^4 Hz using AC impedance spectroscopy and CVs was measured with the speed range from 20 to 200 mV s^{-1} . The CV was scanned at a specific potential to evaluate the stability of the material and the scan range is 1.38 to 1.48 V (vs RHE) with the scan speed is 50 mV s^{-1} and the scan period is 10,000 cycles. In addition, in order to further prove its stability, a constant current test was conducted by chronopotentiometry with a current density of 10 mA cm^{-2} . The Faraday efficiency was evaluated via chronopotentiometry at the current density of 10 mA cm^{-2} and recorded every 15 minutes.

Density Functional Theory (DFT) Calculations

The present first principle DFT calculations were performed by Vienna Ab initio Simulation Package (VASP) with the projector augmented wave (PAW) method.^{2,3} The

exchange-functional is treated using the generalized gradient approximation (GGA) of Perdew-Burke-Ernzerhof (PBE) functional.⁴ All of the structures were spin polarized. The energy cutoff for the plane wave basis expansion was set to 520 eV and the force on each atom less than 0.05 eV Å⁻¹ was set for convergence criterion of geometry relaxation. The *k*-points in the Brillouin zone were sampled by a 3×3×1 grid. The self-consistent calculations apply a convergence energy threshold of 10⁻⁵ eV. The DFT-D3 method was employed to consider the van der Waals interaction.⁵ A 15 Å vacuum was added along the *z* direction in order to avoid the interaction between periodic structures and the bottom layers had been fixed. For Co and Ni atoms, the U corrections had been used in our systems

The free energies were calculated by the equation:⁶ $\Delta G = \Delta E_{\text{DFT}} + \Delta E_{\text{ZPE}} - T\Delta S$, where ΔE_{DFT} is the DFT electronic energy difference of each step, ΔE_{ZPE} and ΔS are the correction of zero-point energy and the variation of entropy, respectively, which are obtained by vibration analysis, *T* is the temperature (*T* = 300 K).

- 1 L. Han, X. Y. Yu and X. W. (David) Lou, *Adv. Mater.*, 2016, **28**, 4601–4605.
- 2 G. Kresse and J. Furthmüller, *Comp. Mater. Sci.*, 1996, **6**, 15–50.
- 3 P. E. Blöchl, *Phys. Rev. B*, 1994, **50**, 17953–17979.
- 4 J. P. Perdew, J. A. Chevary, S. H. Vosko, K. A. Jackson, M. R. Pederson, D. J. Singh and C. Fiolhais, *Phys. Rev. B*, 1992, **46**, 6671–6687.
- 5 S. Grimme, J. Antony, S. Ehrlich and H. Krieg, *J. Chem. Phys.*, 2010, **132**, 154104.
- 6 E. Skulason, T. Bligaard, S. Gudmundsdottir, F. Studt, J. Rossmeisl, F. Abild-Pedersen, T. Vegge, H. Jonsson and J. K. Nørskov, *Phys. Chem. Chem. Phys.*, 2012, **14**, 1235–1245.

FIGURES

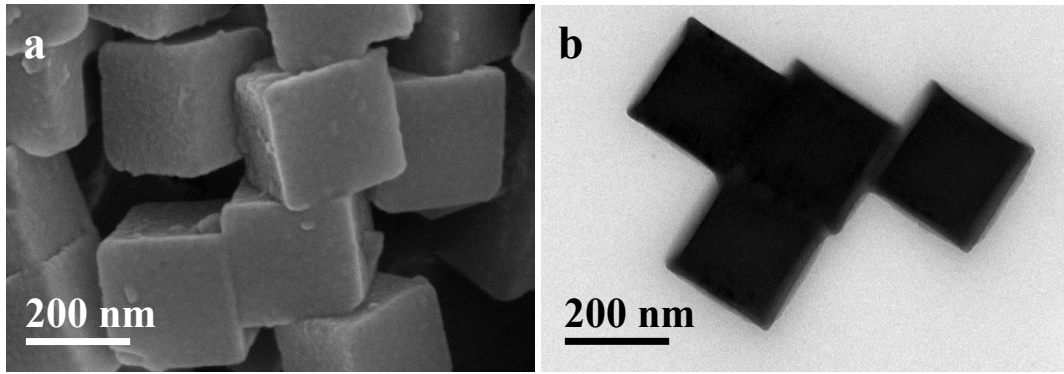


Fig. S1 SEM and TEM images of NiCoPBA Cubes.

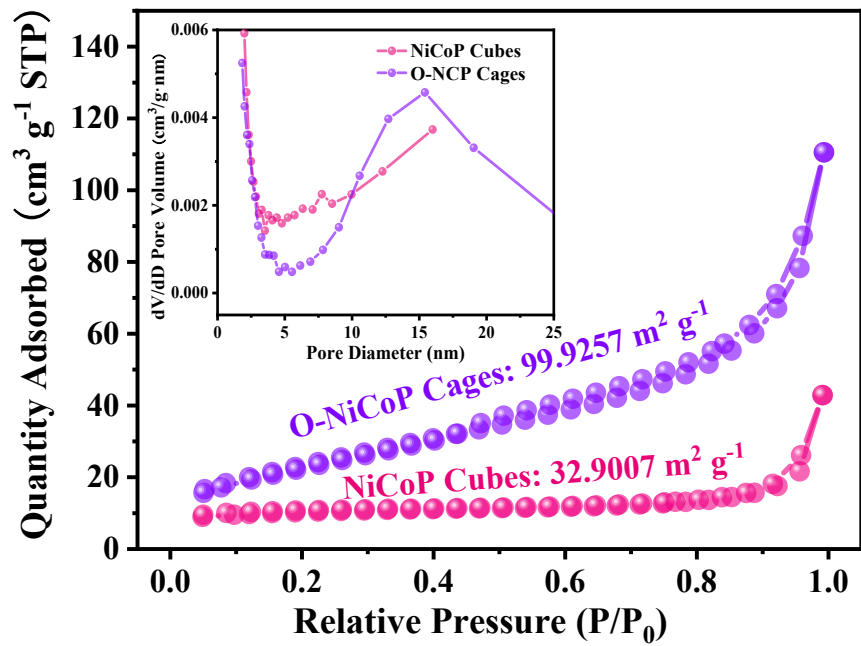


Fig. S2 N_2 adsorption-desorption isotherms and pore size distribution for NiCoP Cubes and O-NiCoP Cages, respectively.

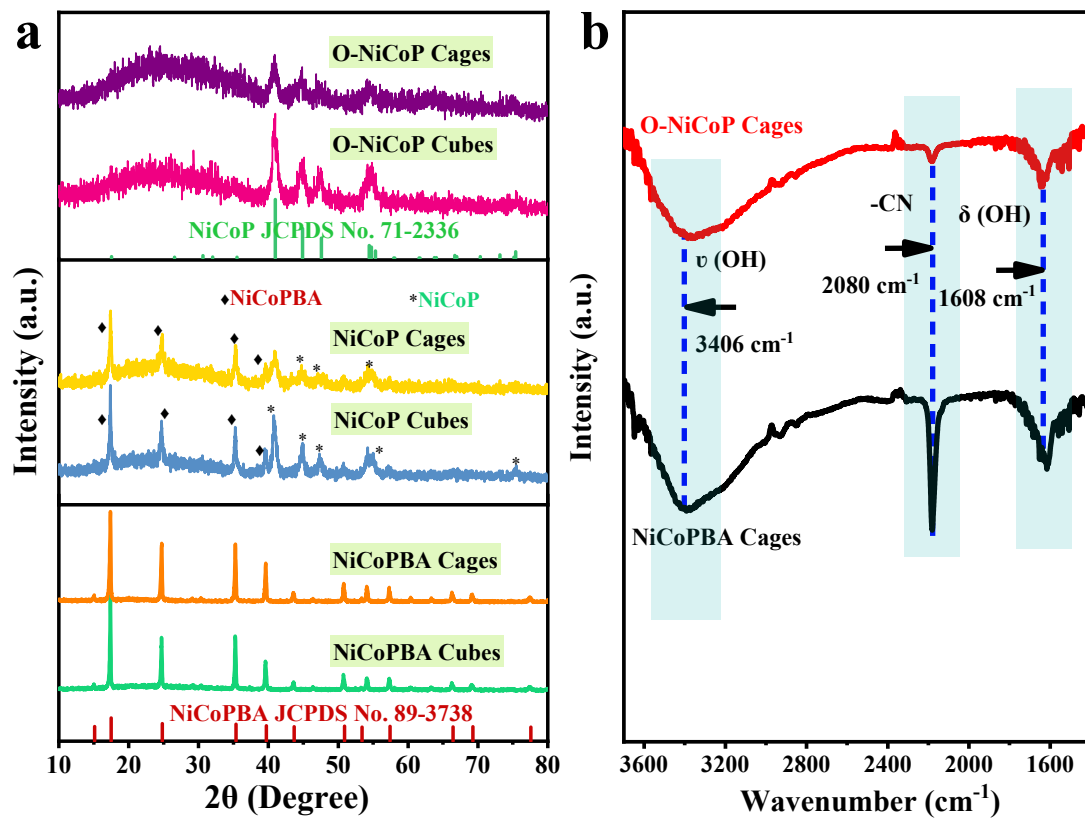


Fig. S3 (a) XRD patterns of NiCoPBA and other derivative catalysts. (b) FT-IR spectra of NiCoPBA Cages and O-NiCoP Cages.

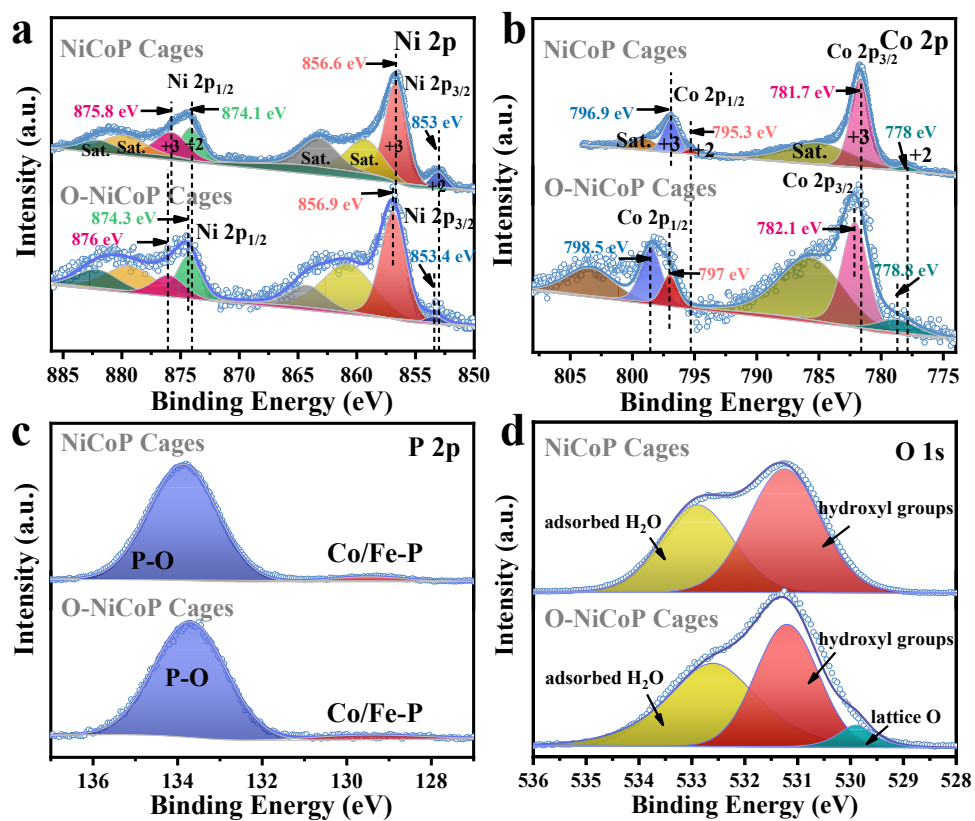


Fig. S4 XPS spectra of NiCoP Cages and O-NiCoP Cages: (b) Ni 2p, (c) Co 2p, (d) P 2p, and (e) O 1s.

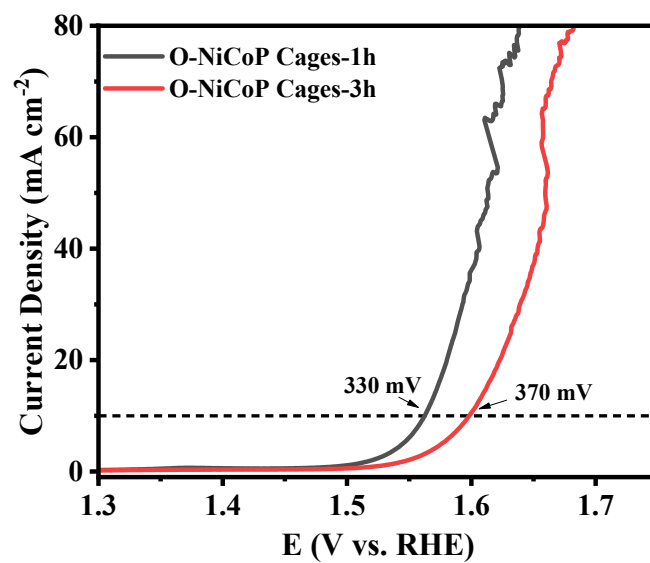


Fig. S5 The LSV curves of O-NiCoP Cages-1h and O-NiCoP Cages-3h samples.

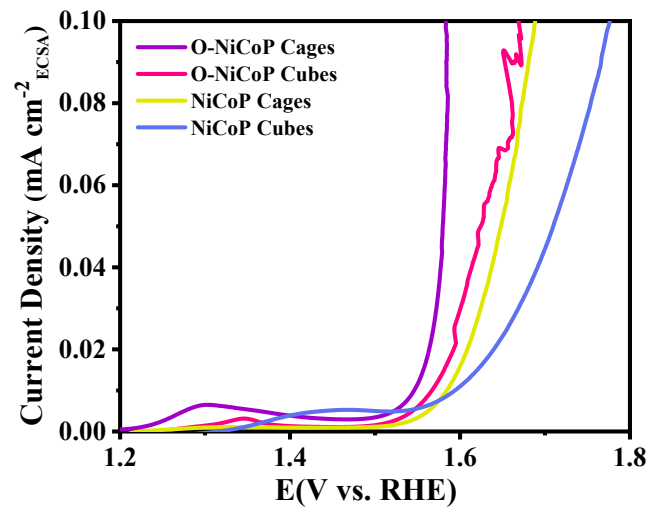


Fig. S6 Polarization curves normalized by the ECSA.

Cyclic Voltammetry testing: Respectively, the voltammetry curves are obtained by cyclic voltammetry experimental method in 1 M KOH that the voltage is from 1.38 V to 1.48 V vs. RHE at the scan rate of 20 mV s⁻¹, 40 mV s⁻¹, 60 mV s⁻¹, 80 mV s⁻¹, 100 mV s⁻¹, 120 mV s⁻¹, 140 mV s⁻¹, 160 mV s⁻¹, 180 mV s⁻¹ and 200 mV s⁻¹. Delta j can be calculated in the voltage of 1.43 V. The slop of these pots at different scan rate is related to electrochemically active surface area.

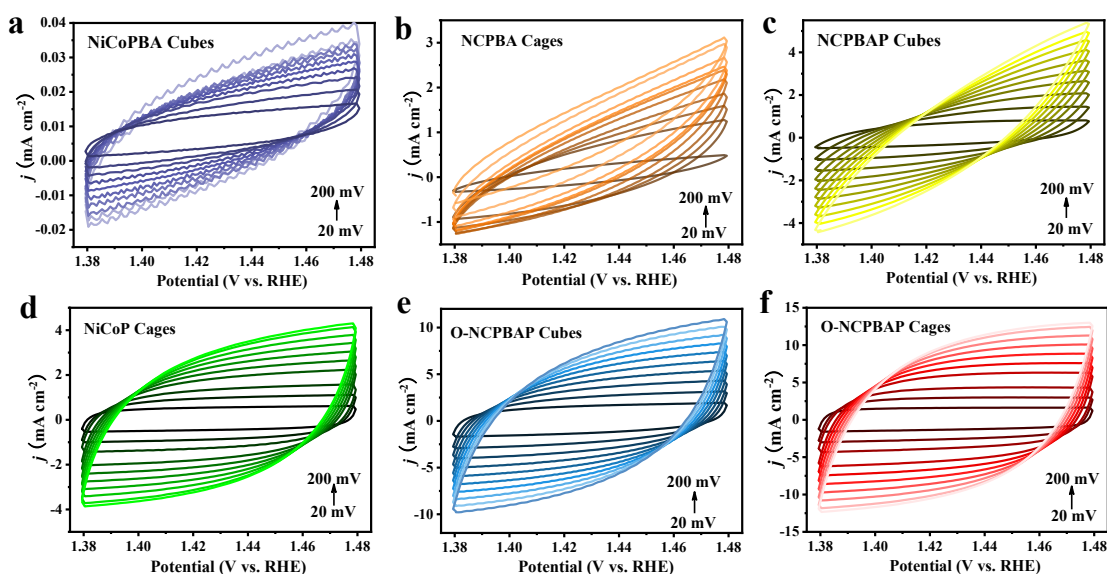


Fig. S7 CVs of sample (a) NiCoPBA Cubes, (b) NiCoPBA Cages, (c) NiCoP Cubes, (d) NiCoP Cages, (e) O-NiCoP Cubes, and (f) O-NiCoP Cages in 1 M KOH between 1.38 V and 1.48V vs. RHE.

The turnover frequency (TOF) calculation: By using the previous reported method to calculate the active sites and TOF of NCPBA Cubes and O-NCPBAP Cages. In order to calculate the active sites for each catalyst, CV measurements with potential window from 0.4 V to 1.0 V were carried out in phosphate buffered saline (PBS, pH= 7), where we assumed that no oxygen evolution reaction together with electrochemical corrosion of our samples happened. The turnover frequency (TOF) can be calculated with the following equation:

$$\text{TOF} = I/Q$$

Where I (A) is the current of the polarization curve, we obtained it from the LSVs measurements. Voltammetric charges (Q) is calculated by the following equation:

$$Q = 4Fn$$

Where F is Faraday constant (96480 C mol⁻¹), n is the number of active sites. In the experiment, the voltammetry curve is obtained by CVs measurements with phosphate buffer (pH = 7) at a scan rate of 50 mV s⁻¹. The voltammetric (Q) is obtained after deduction of the blank value.

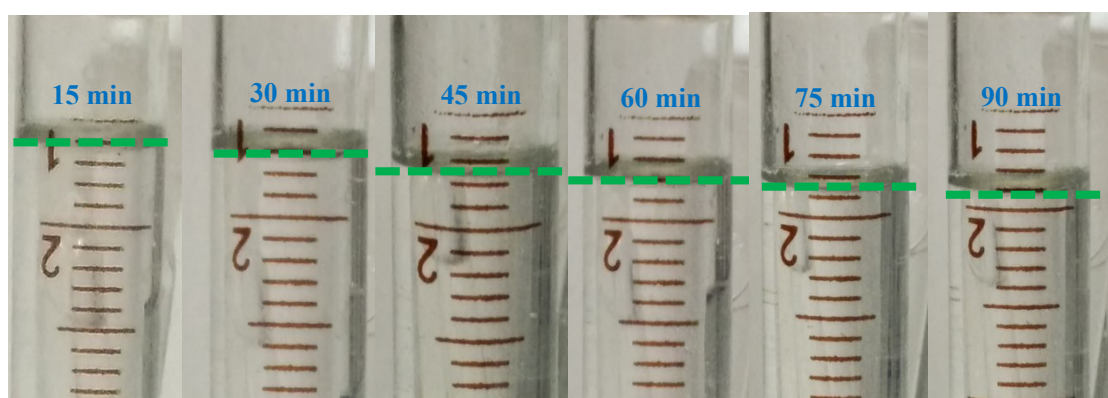
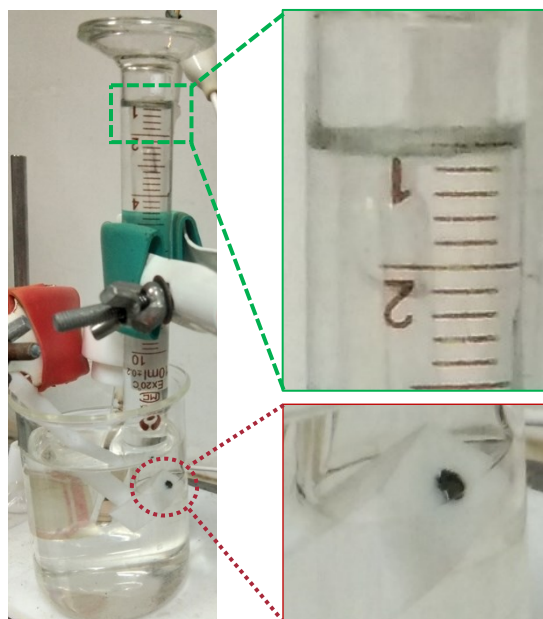


Fig. S8 A digital photograph showing the continuous generation of O₂ bubbles on the O-NiCoP Cages catalyst.

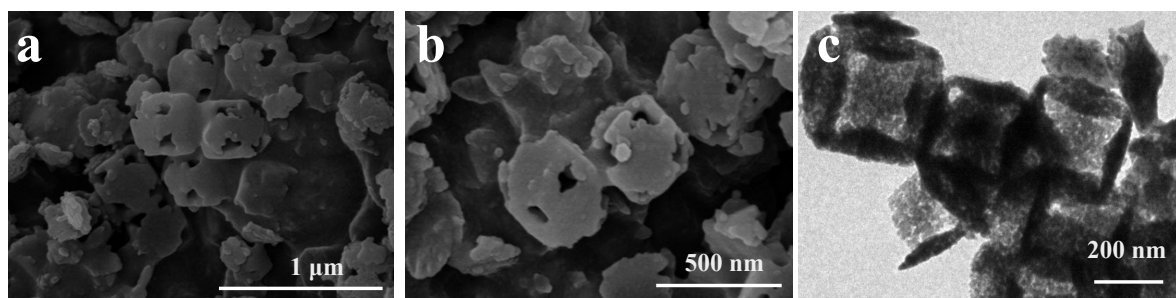


Fig. S9 SEM and TEM images of O-NiCoP Cages after OER test.

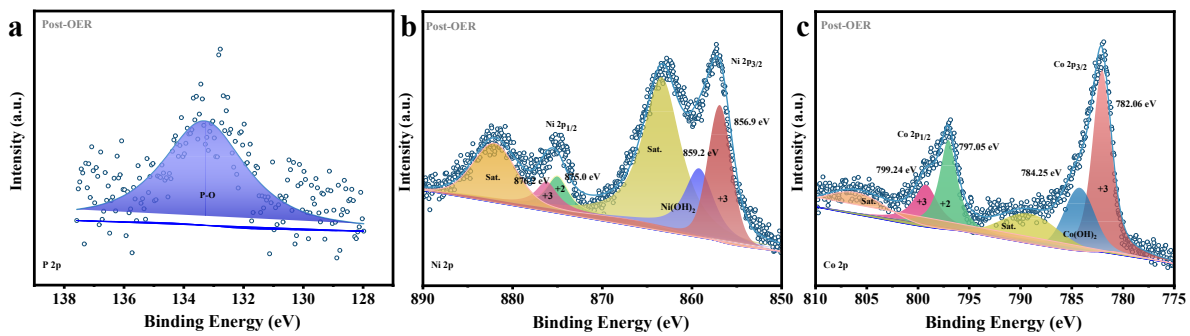


Fig. S10 XPS spectra of O-NiCoP Cages after OER test: (a) P 2p, (b) Ni 2p, (c) Co 2p.

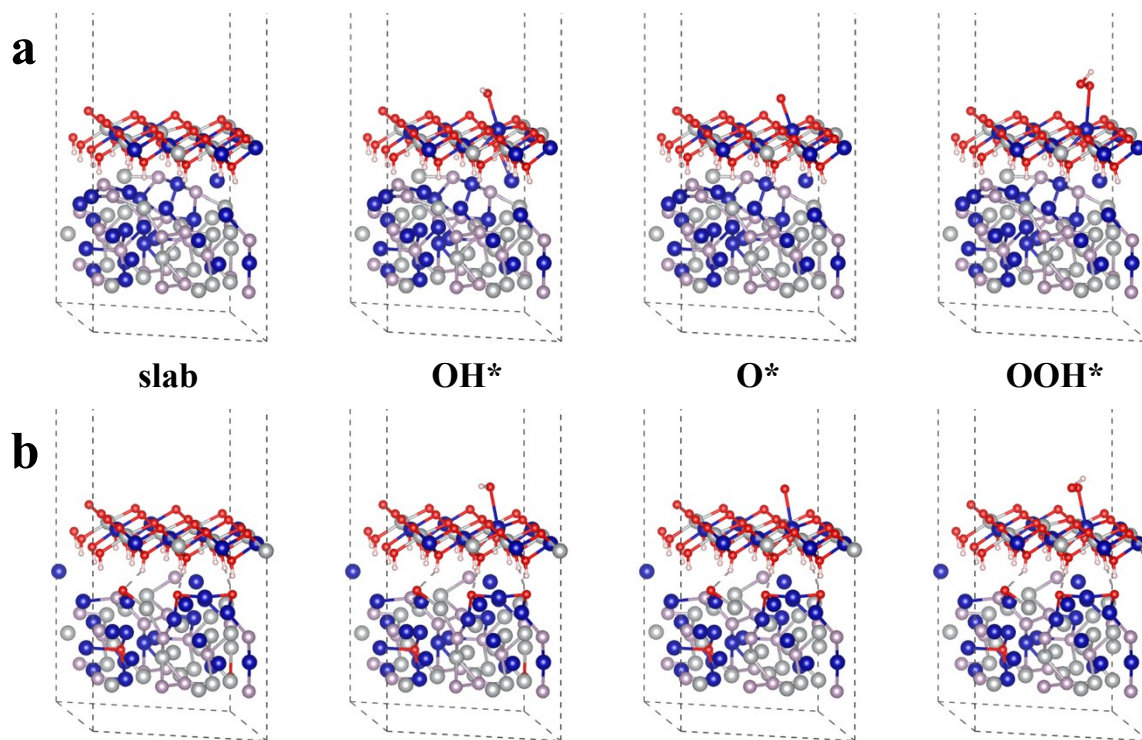


Fig. S11 Simulated OER steps proceeded at oxyhydroxides site on (a) NiCoOOH/NiCoP and (b) NiCoOOH/O-NiCoP models. The blue, gray, purple, red and pink balls represent Co, Ni, P, O and H, respectively.

Table S1 Summary of electrochemical OER performance of previously reported metal phosphide.

Catalyst	η_{10}/mV	Test condition	Ref.
CoP NR/C	320	1M KOH	4
Ni-P film	344	1M KOH	5
CoMnP	330	1M KOH	6
Ni ₂ P	320	1M KOH	7
NiCoP/C	330	1M KOH	8
NiMoP ₂	330	1M KOH	9
Al-Doped CoP nanoarray	330	1M KOH	10
CoMn-P-3DHFLMs	318	1M KOH	11
Fe ₁ Co ₁ -P/C	360	1M KOH	12
Ni ₅ P ₄	330	1M KOH	13
CP@FeP	365	1M KOH	14
CoP hollow polyhedra	400	1M KOH	15
CoP MNA	310	1M KOH	16
This work	310	1M KOH	

- 7 J. F. Chang, Y. Xiao, M. L. Xiao, J. J. Ge, C. P. Liu and W. Xing, *ACS Catal.*, 2015, **5**, 6874–6878.
- 8 N. Jiang, B. You, M. L. Sheng and Y. J. Sun, *ChemCatChem*, 2016, **8**, 106–112.
- 9 P. L. He, X. Y. Yu and X. W. Lou, *Angew. Chem. Int. Ed.*, 2017, **56**, 3897–3900.
- 10 D. Li, H. Baydoun, C. N. Verani and S. L. Brock, *J. Am. Chem. Soc.*, 2016, **138**, 4006–4009.
- 11 Q. Wang, Z. Q. Liu, H. Y. Zhao, H. Huang, H. Jiao and Y. P. Du, *J. Mater. Chem. A*, 2018, **6**, 18720–18727.
- 12 X. D. Wang, H. Y. Chen, Y. F. Xu, J. F. Liao, B. X. Chen, H. S. Rao, D. B. Kuang and C. Y. Su, *J. Mater. Chem. A*, 2017, **5**, 7191–7199.
- 13 R. Zhang, C. Tang, R. M. Kong, G. Du, A. M. Asiri, L. Chene and X. P. Sun, *Nanoscale*, 2017, **9**, 4793–4800.
- 14 G. L. Li, X. B. Zhang, H. Zhang, C. Y. Liao and G. B. Jiang, *Appl. Catal. B-Environ.*, 2019, **249**, 147–154.
- 15 W. Hong, M. Kitta and Q. Xu, *Small Methods*, 2018, **2**, 1800214.
- 16 M. Ledendecker, S. K. Calderín, C. Papp, H. P. Steinrück, M. Antonietti and M. Shalom, *Angew. Chem. Int. Ed.*, 2015, **54**, 12361–12365.
- 17 D. H. Xiong, X. G. Wang, W. Lia and L. F. Liu, *Chem. Commun.*, 2016, **52**, 8711–8714.
- 18 M. J. Liu and J. H. Li, *ACS Appl. Mater. Interfaces*, 2016, **8**, 2158–2165.
- 19 Y. P. Zhu, Y. P. Liu, T. Z. Ren and Z. Y. Yuan, *Adv. Funct. Mater.*, 2015, **25**, 7337–7347.